Inorganic Chemistry

Article

pubs.acs.org/IC

The Curious Case of Mesityl Azide and Its Reactivity with bpyNiEt$_2$

Brooke M. Otten, Travis M. Figg, and Thomas R. Cundari*

Department of Chemistry, Center for Advanced Scientific Computing and Modeling, University of North Texas, 1508 Mulberry, Denton, Texas 76203, United States

Supporting Information

ABSTRACT: A DFT analysis of the reaction of bpyNiEt$_2$ with ArN$_3$ was performed for *para*-tolyl-azide (Ar = pTol), 3,5-dimethyl-phenyl-azide (Ar = mXy) and *ortho*-tolyl-azide (Ar = oTol), and mesityl-azide (MesN$_3$). Of particular interest were the different products obtained for the latter (ethylene, butane, azomesitylene, mesityl-ethylamine, etc.) versus the other reagents, i.e., (bpyNi(N(Ar)Et)(Et)). Calculated thermodynamics and kinetics for metal-free reactions did not differentiate MesN$_3$ from the other aryl azides. Once ^{2}bpyNiEt$^\bullet$ was generated via bond homolysis, formation of ethylene by β-H elimination was facile, as was formation of nickel-imidyl (NR$^{-\bullet}$) intermediates by reaction of ArN$_3$ with bpyNiEt$_x$ (x = 0−2). On the basis of computed energetics, three reactions of bpyNiEt$_2$ were proposed to compete: Ni−C bond homolysis, reductive elimination of butane, and nucleophilic attack (NA) by ArN$_3$. Inspection of their temperature dependence suggested that NA and Ni−Et bond homolysis dominated at lower and higher temperatures, respectively. Calculated Ni−N and Ni−C bond dissociation free energies (BDFEs) suggested the role of radical pathways in discriminating bpyNiEt$_2$/ArN$_3$ reactions, and implied that the concentration of radicals such as aminyl (ArN$^\bullet$(Et)), ^{2}bpyNiEt$^\bullet$, and Et$^\bullet$ will be greatest for MesN$_3$.

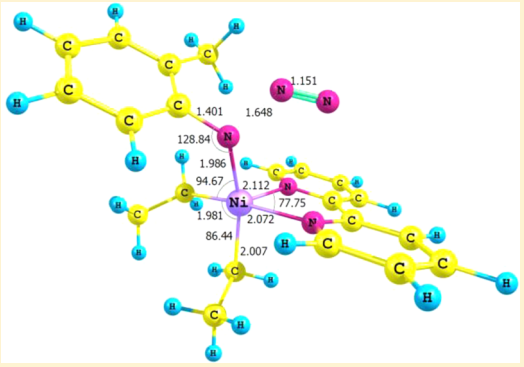

INTRODUCTION

At the same time as the original reports of N_2O oxy-insertion reactivity with nickel organometallics,[1] Hillhouse et al. described similar chemistry with aryl azides (ArN$_3$) leading to C—N bond formation, an important reaction in its own right. There is considerable interest in the organic synthesis community in developing more direct catalytic routes to C—N bond formation without the need for multistep halogenation/bond coupling protocols. Furthermore, Hillhouse et al. reported an interesting dichotomy in observed reactivity. To wit, *para*-tolyl-azide (pTolN$_3$), 3,5-dimethyl-phenyl-azide (mXyN$_3$), and *ortho*-tolyl-azide (oTolN$_3$) reacted with bpyNiEt$_2$ (Et = ethyl, bpy =2,2′-bipyridine) to form the Ni^{II}-amide product expected from insertion of aryl-nitrene (ArN) into a Ni—C$_{Et}$ bond: bpyNi(Et)(N(Et)Ar).[2] However, mesityl azide (MesN$_3$) gave butane, ethylene, and other nitrogen-containing products such as MesN(Et)H and MesN=NMes.[3]

The most obvious difference between MesN$_3$ and other aryl azide reagents is the greater steric profile of the former due to the existence of two methyl groups *ortho* to the azide moiety. As methyl groups are electron-donating, one would expect a mesityl to be more electron-rich than its mono- and dimethyl counterparts. Potentially opposing the latter proposal is work by Yamamoto and Abla that indicated electron-withdrawing substituents on arenes facilitated reductive elimination in bpy-ligated Ni^{II}-dialkyl complexes.[4] Temperature effects may also play a role given that the syntheses were carried out at different temperatures: −78 °C, 0 °C, and room temperature.[3,4] Competing processes that could explain the experimental products include reactions that are entropy favored (homolytic Ni−C bond scission, bpyNiEt$_2$ → bpyNiEt$^\bullet$ + Et$^\bullet$), entropy disfavored (S_N2 transition state resulting from attack of ArN$_3$ on bpyNiEt$_2$), and entropy "neutral" (reductive elimination transition state emanating from bpyNiEt$_2$).

These intriguing experimental results, in conjunction with the importance of carbon−nitrogen bond forming reactions in organic synthesis, led us to initiate a DFT study of the reaction of aryl azides with bpyNiEt$_2$. The thermodynamics and kinetics of plausible organometallic and organic component reactions were assessed.

RESULTS

1. Geometry of MesN$_3$. The B3LYP/6-31+G(d)-optimized geometry of MesN$_3$ (Figure 1) was distinct from other aryl-azides modeled in that the azide moiety was not coplanar with the aryl ring, forming a dihedral of ∼43°. Inspection of the Cambridge Structural Database[5] (n = sample size) showed a median dihedral of 32° (n = 20) for 2,6-disubstituted aryl-azides, greatly reduced to a dihedral of 5° for *ortho*-substituted aryl-azides (n = 29) and aryl azides with only hydrogen atoms in the 2 and 6 positions (n = 57). Hence, computed geometries, corroborated by crystallography, provided evidence for the steric hindrance impacted upon the azide moiety by 2,6-disubstitution of an aryl group.

Received: July 25, 2014
Published: October 17, 2014

   dx.doi.org/10.1021/ic501766k | *Inorg. Chem.* 2014, 53, 11633−11639

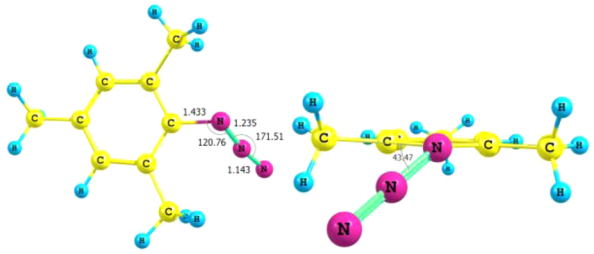

Figure 1. Two views of DFT-optimized geometry of mesityl azide.

2. Metal-Free Reactions. Computations were first employed to assess whether the experimental differences[3] might be due to intrinsic reactivity differences among the aryl azides. To this end, several prototypical reactions were probed; the first of these was loss of N_2 and formation of a triplet aryl nitrene. Since the N_2 expulsion involves a "spin flip", minimum energy crossing points (MECPs) were computed via the method of Besora and Harvey.[6] Dimerization of ArN_3 to yield azo compounds and 2 equiv of dinitrogen was also modeled. Finally, reaction of aryl azides with ethyl radical (which may be generated by Ni−C bond homolysis) was investigated. In each case, these reactions were found to be thermodynamically and kinetically viable and, more importantly, do not distinguish among $pTolN_3$, $mXyN_3$, $oTolN_3$, and $MesN_3$. The detailed results of these metal-free reactions can be found in Supporting Information.

3. Organometallic Reactions. Given that metal-free reactions of $pTolN_3$, $mXyN_3$, $oTolN_3$, and $MesN_3$ did not suggest any inherent difference in their reactivity, we focused our attention on modeling metal based reactions. In general, the reactions can be subdivided into 3 domains: those that involve initial (a) Ni−C bond homolysis, (b) reductive elimination of butane, and (c) nucleophilic attack of NAr_3 on $bpyNiEt_2$.

a. Initial Ni−C Bond Homolysis. i. $bpyNiEt_2$ → $bpyNiEt^{\bullet}$ + $Et^{\bullet}$. The DFT-optimized geometry of $bpyNiEt_2$ is shown in Figure 2. Calculation of the Ni−C homolytic BDE (bond

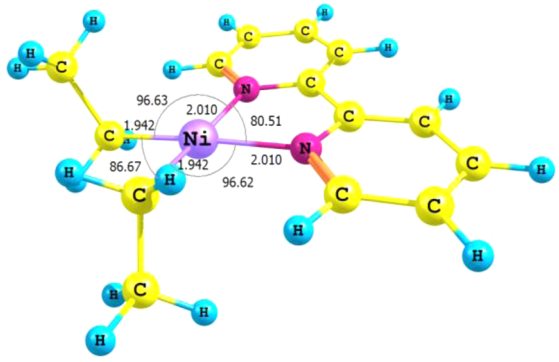

Figure 2. DFT-optimized singlet ground state of $bpyNiEt_2$. Bond lengths and bond angles in this and subsequent structures are given in Å and degrees, respectively.

dissociation enthalpy) and BDFE of $bpyNiEt_2$ yielded ΔH_{diss} = 34.2 and ΔG_{diss} = 18.1 kcal/mol, respectively, at 298.15 K. *Since ΔG approaches ΔH at lower temperatures, homolytic bond dissociation of a Ni−C bond in $bpyNiEt_2$ is expected to become more favorable as the temperature is increased.* The calculated BDFE at 298.15 of 18.1 kcal/mol is well below the calculated ΔG_{MECP} of ∼35 kcal/mol (see Supporting Information) for N_2 loss from ArN_3 to produce ^3ArN.

ii. β-Hydrogen Elimination from $bpyNiEt^{\bullet}$. To probe the experimentally observed formation of ethylene, β-H elimination from $^2bpyNiEt^{\bullet}$ was investigated, Scheme 1. Calculations

Scheme 1. DFT-Calculated Energies (kcal/mol) for β-Hydrogen Elimination from $bpyNiEt^{\bullet}$

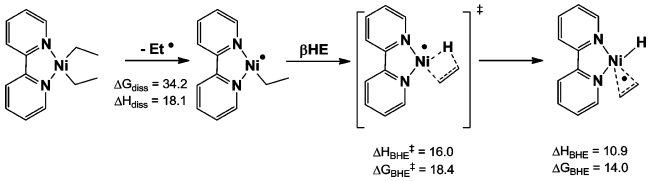

assumed that ethylene was formed after Ni—C bond homolysis from $bpyNiEt_2$ to produce an open coordination site for β-H elimination (BHE). BHE was calculated to be endergonic by 14.0 kcal/mol (ΔH_{BHE} = 10.9 kcal/mol). For the $^2bpyNi(H)(\eta^2\text{-}C_2H_4)$ product the C═C bond axis was perpendicular to the square plane of nickel. A β-agostic conformer of $^2bpyNiEt^{\bullet}$ (C_s minimum) was isolated in which the N_{bpy}—Ni—C—C dihedrals are 0° and 180°, but this conformer was 5.9 kcal/mol higher in free energy than the lowest energy $^2bpyNiEt^{\bullet}$ conformer.

A β-H elimination TS was also isolated, with calculated $\Delta H_{BHE}^{\ddagger}$ = 16.0 kcal/mol and $\Delta G_{BHE}^{\ddagger}$ = 18.4 kcal/mol versus $^2bpyNiEt^{\bullet}$, Scheme 1. Values computed here for bipyridine-supported β-H elimination are similar to those reported by Kogut et al. (Figure 3) in a joint theory−experiment study of a

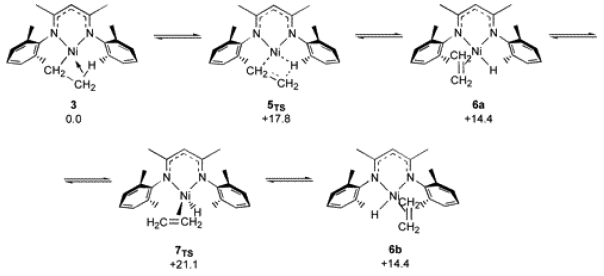

Figure 3. DFT-calculated free energies (kcal/mol) for β-hydrogen elimination from β-diketiminate-Ni-ethyl, taken from ref 7.

β-diketiminate-Ni-ethyl complex.[7] The β-H elimination TS was 18.4 kcal/mol above $^2bpyNiEt^{\bullet}$, which was in turn 18.1 kcal/mol above $bpyNiEt_2$. Hence, we cannot rule out alternative routes to the experimentally observed ethylene.

ii. Reaction of Aryl Azides with $^2bpyNiEt^{\bullet}$. Given the facility with which $^2bpyNiEt^{\bullet}$ is computed to be generated at 298.15 K, its reactivity with aryl azides was of interest. This organometallic radical has a calculated spin density of 1.2 e^- on the Ni, −0.2 e^- on C_α of the ethyl ligand and little spin density elsewhere. Homolytic scission of the Ni−Et bond will produce two radicals, $Et^{\bullet}$ and $^2bpyNiEt^{\bullet}$. The former was expected to be more reactive, and indeed calculations backed this supposition as discussed in the Supporting Information. In this section the focus is on the reaction of the organometallic radical with aryl azides. The displacement reaction ArN_3 + $^2bpyNiEt^{\bullet}$ → $^2bpyNi(NAr)Et^{\bullet}$ + N_2 had calculated $\Delta H^{\ddagger}$ = −4.4 kcal/mol and $\Delta G^{\ddagger}$ = 9.6 kcal/mol for Ar = Ph. An organometallic variant of a 3,3-triazenyl radical (i.e., $^2bpyNiEt(Ph)NNN^{\bullet}$) that might

dx.doi.org/10.1021/ic501766k | Inorg. Chem. 2014, 53, 11633−11639

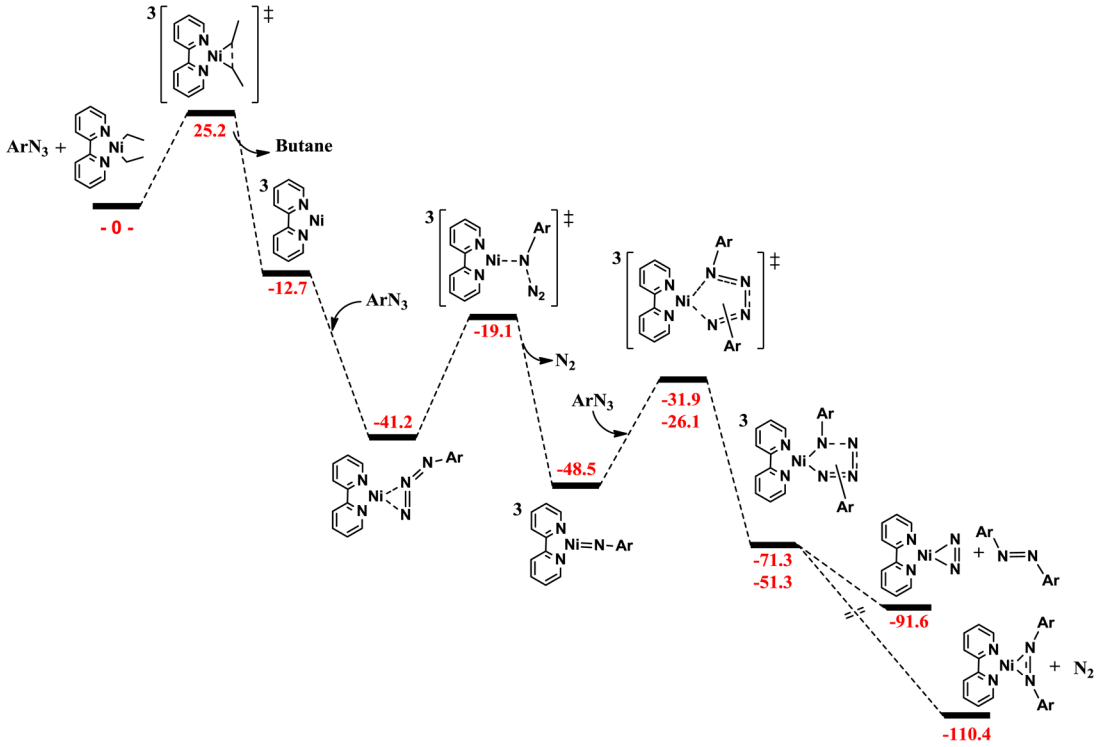

Figure 4. Reaction coordinate for the formation of a nickel-imidyl complex (^{3}bpyNi═NAr) and its reaction with ArN_3 (Ar = Ph). Free energies (kcal/mol, in red) were calculated at 298.15 K and 1 atm. Triplet stationary points are indicated by a superscript, prefix "3". The remaining stationary points were calculated to be more stable as singlets. For 1,3-dipolar addition TSs and their diazenido products, the top values refer to the free energies for the regiochemistry leading to 1,4-diazenido product and the lower values are for the 1,2-diazenido pathway.

precede this TS was not sought, but the non-negligible barrier to N_2 loss implied, quite reasonably, that aryl azides will react more readily with ethyl radical than ^{2}bpyNiEt$^\bullet$, producing aminyl radicals, ArN$^\bullet$(Et). Aminyl radicals have computed relatively weak N−H bond dissociation enthalpies of ∼81−82 kcal/mol for the different Ar modeled, and so presumably are relatively stable radicals that may then rebound back on to ^{2}bpyNiEt$^\bullet$ to give bpyNi(Et)(N(Ar)Et) products.

b. Initial Reductive Elimination. i. bpyNiEt$_2$ → ^{3}[RE]‡ → ^{3}bpyNi + Butane. Yamamoto and Alba reported a Hammett study of the impact of ArX solvent on reductive elimination from bpyNiEt$_2$.[4] They concluded that electron-withdrawing X groups facilitated butane formation, and proposed a mechanism involving charge transfer from bpyNiEt$_2$ to ArX.[4] This mechanism implies association, perhaps weak, between bpyNiEt$_2$ and arene moieties. Three modes of reactant interaction immediately suggested themselves: (a) π−arene stacking between ArN_3 and bpy, (b) Ni−π arene interaction, and (c) ligation of ArN_3 through a N lone pair. Calculations at both the B3LYP/6-31+G(d) and M06/6-31+G(d) level of theory, the latter indicated to be better than the former at modeling weak interactions,[8] *did not* indicate the intermediacy of bound bpyNiEt$_2$·ArN_3 adducts.

Reductive elimination from bpyNiEt$_2$ to produce butane and triplet bpyNi was mildly endothermic, but exergonic: ΔH_{RE} = +0.6, ΔG_{RE} = −12.7 kcal/mol at 298.15 K. The *calculated reductive elimination barrier was* $\Delta H_{RE}^‡$ *= 26.9,* $\Delta G_{RE}^‡$ *= 25.2 kcal/mol at 298.15 K.* This barrier was ∼10 kcal/mol lower than the calculated singlet−triplet MECPs for N_2 loss from ArN_3 (Supporting Information). Similarity in the calculated enthalpy and free energy barriers for butane reductive elimination implied minimal temperature dependence for the reaction. Reductive elimination of butane from bpyNiEt$_2$ entails a spin crossing. Calculation of the MECP for butane reductive elimination puts it 11 kcal/mol lower in free energy than the triplet TS and more similar in geometry to the triplet than singlet reductive elimination TS.

ii. Formation of Ni−Imidyl Complexes. The energetics of reactions leading to bpyNi═NPh were initially explored for the parent phenyl azide. As with other reactions in which N_2 was produced, formation of a nickel−imide from bpyNiEt$_2$ and ArN_3 was calculated to be both highly exothermic and highly exergonic: ΔH = −62.2, ΔG = −76.0 kcal/mol at 298.15 K for ArN_3 + bpyNiEt$_2$ → ^{3}bpyNi═NAr + butane + N_2 (Ar = Ph). The ^{3}bpyNi═NAr intermediates were calculated to be triplets, albeit slightly (for example, ΔG_{ST} = 2.5 kcal/mol, Ar = Ph), in contrast to diamagnetic ground states for (P∼P)Ni═NAr species (P∼P ≡ chelating bis-phosphine).[9] The ^{3}bpyNi═NPh complex was trigonal planar about Ni, with a calculated NiN bond length for the imide ligand of 1.718 Å. Substituted bpyNi═NAr species were also calculated to have triplet ground states, trigonal planar Ni coordination, and NiN_{imide} bond lengths of ∼1.72 Å. Computed bond lengths to the imide ligands compared well with nickel−nitrogen bonds in three-coordinate nickel imides of 1.662 Å (β-diketiminate−Ni−NAd) as well as 1.702, 1.703, and 1.673 Å for three (dtbpe)Ni═NiR complexes where R = Dipp, Mes, and Ad, respectively; dtbpe =1,2-bis(di-*tert*-butylphosphino)ethane, Dipp =2,6-di-isopropyl-phenyl, Ad = 1-adamantyl.[9−11]

The spin density (Supporting Information Figure S-1) has ^{3}bpyNi═NPh with 0.9 unpaired e^- on Ni, and 0.8 unpaired e^- on the imide N, with the remainder delocalized onto the phenyl substituent. This delocalization is consistent with the short calculated N_{imide}—C_{ipso} distance of 1.333 Å. Furthermore, as

dx.doi.org/10.1021/ic501766k | *Inorg. Chem.* 2014, 53, 11633−11639

discussed by Figg et al. for related oxyl ($O^{-\bullet}$) complexes,[9] and for β-diketiminate—Ni—NR complexes,[12] this disposition of spin density implies an imidyl ($NR^{-\bullet}$) description for ^{3}bpyNi=NPh.

iii. Formation of Ni–Imidyl Complexes from ^{3}bpyNi. Experimentally observed formation of azo compounds, ArN=NAr, suggested intermediacy of free or ligated nitrenes. Hence, pathways leading to and from ^{3}bpyNi=NPh were modeled. The computed pathways were similar to those reported by Harold and co-workers for isolated (P~P)nickel-imides.[13] The first series of imide-forming reactions utilized ^{3}bpyNi as the model reagent, Figure 4. As expected for an unsaturated organometallic, reactions with PhN_3 were highly exergonic. The most stable linkage isomer was bpyNi(η^2-*N*,*N*-N_3Ph) with a three-membered NiN_2 ring, Figure 5, and this was

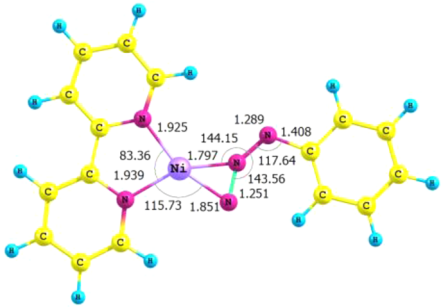

Figure 5. DFT-optimized structure of bpyNi(η^2-*N*,*N*-N_3Ph).

exergonic by 28.5 kcal/mol relative to separated ^{3}bpyNi and PhN_3. Loss of dinitrogen from bpyNi(η^2-*N*,*N*-N_3Ph) to form ^{3}bpyNi=NPh was exergonic by an additional 34.8 kcal/mol. *Hence, calculations suggested that once the barrier to reductive elimination of butane from bpyNiEt$_2$ is surmounted to form ^{3}bpyNi, a series of facile, highly exergonic reactions resulted in an imidyl, ^{3}bpyNi=NAr, and N_2.*

iv. 1,3-Dipolar Addition of PhN_3 to ^{3}bpyNi=NPh. In light of previous research,[12] 1,3-dipolar addition of PhN_3 to ^{3}bpyNi=NPh was studied. Two regiochemistries for the cycloaddition are possible, leading to either a 1,2- or 1,4-tetrazenido intermediate. Structurally characterized tetrazenido complexes possess 1,4-regiochemistry.[14−17] The 1,2-regiochemistry is likely unstable with respect to expulsion of N_2 and formation of an azo complex, e.g., bpyNi(η^2-PhNNPh). Note that other plausible products of decomposition of bpyNi(κ^2-*N*,*N*-PhN_4Ph) → ^{1}bpyNi(N_2) + PhN=NPh versus ^{1}bpyNi(η^2-PhNNPh) + N_2 were compared, and revealed a calculated 18.8 kcal/mol advantage (ΔG) for the latter, Figure 4.

The 1,4-tetrazenido complex was exergonic by 22.8 kcal/mol relative to ^{3}bpyNi=NPh and PhN_3. The 1,3-dipolar addition TS to this tetrazenido complex had $\Delta H_{1,3}^{\ddagger}$ = 3.7 kcal/mol and $\Delta G_{1,3}^{\ddagger}$ = 16.6 kcal/mol at 298.15 K, Figure 4. The formation of the 1,2-tetrazenido was disfavored kinetically and thermodynamically. *Thus, in a cascade of reactions starting from bpyNiEt$_2$, the original reductive elimination to make butane was the calculated rate-determining step in the formation of bpyNi-imidyl complexes.* As such, one would expect that such a pathway would not discriminate among the various aryl azides. Indeed, calculation of the reaction coordinate in Figure 4 for Ar = Mes showed nearly identical free energies as were calculated for Ar = Ph.

c. Nucleophilic Attack. i. ArN_3 + bpyNiEt$_2$ → ^{1,3}[NA]‡ → ^{1,3}bpyNi(Et)$_2$(=NAr) → ^{1,3}[Mig]‡ → bpyNi(Et)(N(Ar)Et). On the basis of a previous computational study of the reactivity of bpyNi^{II}-dialkyls with nitrous oxide,[18] the mechanism shown in Scheme 2 was modeled. The TSs for NAr insertion into the

Scheme 2. Proposed Pathway for Nickel-Mediated Aryl Nitrene Insertion into a Nickel−Carbon Bond

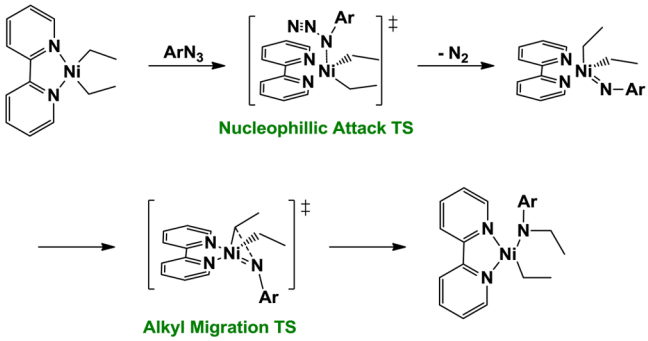

Ni−C bond (alkyl migration) were calculated to be singlets (triplets are ca. 12 kcal/mol higher for the various Ar) and well below the TSs for nucleophilic attack (NA) discussed below. Hence, the discussion below will focus on the NA step of the mechanism. As an aside, barriers to butane reductive elimination from bpyNi(Et)$_2$(=NAr) were much higher than barriers to ethyl migration to make amide products.

After analysis of singlet and triplet transition states, in a variety of coordination and conformational isomers, the lowest energy NA transition states were found to be triplets. The TS for oTolN_3 addition to bpyNiEt$_2$ is shown in Figure 6. Several

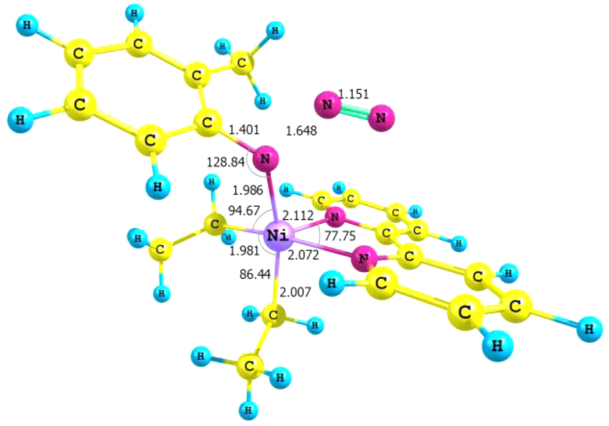

Figure 6. DFT-optimized triplet transition state for N_2 loss from bpyNi(Et)$_2$(oTolN_3).

features are of interest. First, coordination about Ni was close to square pyramidal, with one of the bpy arms in the apical position. Hence, the incipient imidyl ligand occupied a basal coordination site. Second, the coordination geometry of the TS required a significant deformation of the ground state nickel coordination sphere of bpyNiEt$_2$ such that the bpy and Et ligands were no longer coplanar. Third, the calculated NN distance of the N_2 being expelled was 1.151 versus 1.105 Å for free N_2 at the same level of theory. So, in terms of this metric the NA‡ appears to be "late."

dx.doi.org/10.1021/ic501766k | *Inorg. Chem.* 2014, 53, 11633−11639

The calculated NA transition states are nearly identical energetically, $\Delta G^{\ddagger}_{NA} \sim 30-31$ kcal/mol for the four aryl azides modeled, Table 1, including $MesN_3$. The enthalpic barriers are

Table 1. Calculated Energetics for Nucleophilic Addition (NA) of Aryl Azide to bpyNiEt$_2$

$\Delta H^{\ddagger}_{NA}$ (kcal/mol)	$\Delta G^{\ddagger}_{NA}$ (kcal/mol)	reaction
18.9	31.1	bpyNiEt$_2$ + oTolN$_3$ → ^{3}NA_oTol
19.5	31.0	bpyNiEt$_2$ + pTolN$_3$ → ^{3}NA_pTol
17.4	30.6	bpyNiEt$_2$ + mXyN$_3$ → ^{3}NA_mXy
17.5	30.3	bpyNiEt$_2$ + MesN$_3$ → ^{3}NA_Mes

ca. 12 kcal/mol lower, consistent with a typical $T\Delta S$ contribution for an A + B → C event at STP. As such, the NA reaction will be favored as the temperature is reduced, which is opposite to the temperature effect expected for homolytic bond dissociation of an Ni−C bond in bpyNiEt$_2$.

Singlet and triplet NA transition states were found for all aryl azides, with the typical free energy difference being 3−4 kcal/mol in favor of triplets. As with bpyNiR$_2$/N$_2$O simulations,[18] geometries for singlet and triplet NA‡ are also similar. Fully optimized ^{3}bpyNiEt$_2$ was 12 kcal/mol (ΔG) higher than ground state singlet. The geometry (Figure 7) of ^{3}bpyNiEt$_2$ was

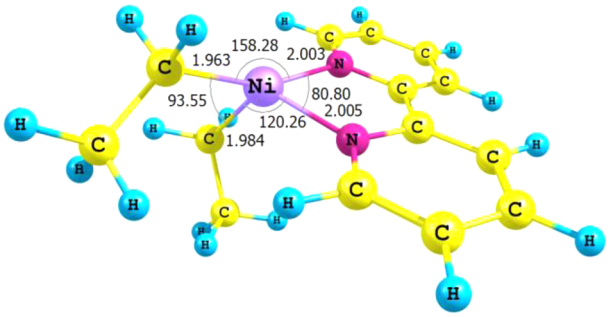

Figure 7. DFT-optimized structure of lowest energy triplet bpyNiEt$_2$.

similar to the bpyNiEt$_2$ fragment contained within the ^{3}NA_oTol transition state. While the singlet ground state of bpyNiEt$_2$ has the square planar geometry expected of a low-spin, d^8 four-coordinate complex (Figure 2), the lowest energy triplet state of ^{3}bpyNiEt$_2$, Figure 7, has a coordination geometry about nickel that is more reminiscent of a trigonal bipyramid with a missing equatorial ligand. Taken together, the various pieces of computational evidence, plus the observed experimental chemistry, imply facile singlet/triplet conversion in this aryl azide chemistry.

DISCUSSION, CONCLUSIONS AND PROSPECTUS

A DFT analysis of the reaction of bpyNiEt$_2$ with ArN$_3$ was performed for *para*-tolyl-azide (Ar = pTol), 3,5-dimethyl-phenyl-azide (Ar = mXy) and *ortho*-tolyl-azide (Ar = oTol), and mesityl-azide (Ar = Mes). Of particular interest were the different products obtained for the latter reagent (ethylene, butane, azomesitylene, etc.) versus the other aryl azides (bpyNi(N(Ar)Et)(Et)). The most important conclusions are collected and discussed in this section.

Computations highlighted the expected chemistry of organic azides as energetic materials. None of the calculated thermodynamics or kinetics for metal-free reactions of ArN$_3$ differentiate MesN$_3$ from the other aryl azides studied experimentally.

The low metal−ligand homolytic bond energies expected of 3d organometallics were manifested in bpyNiEt$_2$. Calculated BDE and BDFE were 34.2 and 18.1 kcal/mol, respectively, at 298.15 K. Hartwig et al. propose that the former reaction enthalpy gives a more accurate estimate of the free energy barrier;[19] within that assumption, $\Delta G^{\ddagger} > \Delta G$ by ∼12 kcal/mol at STP for bond scission, which would be expected to suppress radical pathways engendered by Ni−C scission. Once ^{2}bpyNiEt$^{\bullet}$ was generated via bond homolysis, formation of ethylene via β-H elimination was facile. While a lack of reliable experimental thermochemical data and the well-known difficulties in applying single determinant techniques (including DFT) to 3d metals forestalled calibration of these bond strengths,[20−23] calculations highlight the weak M−C bonds that can lead to radical pathways in 3d metals.

Late metal nitrene/imide/imidyl (L$_n$M(NR)) complexes have been the subject of considerable interest.[7,9−12,24] The ability to exploit their extraordinary reactivity to effect desirable reactions such as the amination of C—H bonds has motivated much of the scrutiny. Lin speculated on the viability of bpy−nickel−imide intermediates in the reactions of bpyNiEt$_2$ with aryl azides.[3] In light of the subsequent success of the same group in isolating low-coordinate imides of nickel,[9] this proposal was quite prescient. The calculations predicted a triplet ground state for bpyNi═NAr, although singlet states were close in energy. Formation of nickel-imidyl (NR$^{-\bullet}$) intermediates by reaction of ArN$_3$ with bpyNiEt$_x$ (x = 0−2) was calculated to be thermodynamically and kinetically facile. Description of these NR-ligated complexes as imidyls is more than semantics vis-à-vis the challenges faced in functionalization of strong C—H bonds. Transformations such as M(═E)R → MER are thwarted by the polarity of the M$^{\delta+}$═E$^{\delta-}$ and M$^{\delta+}$—X$^{\delta-}$ bonds. Brown and Mayer discuss the need to make the oxo ligand (M = Re, E = O, X = Ph) more electrophilic in a study of the M(═E)X → MEX reaction.[25] For late transition metals, greater imidyl character for L$_n$M(NR) complexes implies a decrease in nucleophilicity at the nitrogen versus the imide (NR^{2-}) descriptions of earlier, more electropositive transition metals.[26]

DFT calculations on the reaction ArN$_3$ + bpyNiEt$_2$ → bpyNi(Et)(N(Ar)Et) supported a mechanism similar to that proposed by Figg et al. for the bpyNiEt$_2$/N$_2$O reaction.[18] Surprisingly, calculated energetics for the modeled reaction pathways did not indicate a significant difference among the ArN$_3$ modeled. Free energies for the computed rate-determining step, nucleophilic attack (NA) of the internal N of ArN$_3$ on bpyNiEt$_2$, were nearly constant as a function of Ar at ∼31 kcal/mol.

On the basis of computed energetics, three reactions were proposed to compete: Ni−C homolytic bond dissociation from bpyNiEt$_2$, reductive elimination of butane from the same organonickel complex, and nucleophilic attack of bpyNiEt$_2$ on ArN$_3$. Using the Gibbs equation, it was assumed G(0 K) ≡ H(298.15 K), G(298.15 K) ≡ G(300 K), and then from these two end points G(100 K) and G(200 K) values were linearly interpolated. The data thus obtained are plotted in Figure 8. Given the similarity in computed nucleophilic attack barriers, data are plotted only for the oTolN$_3$/bpyNiEt$_2$ couple.

Inspection of the temperature dependence of butane reductive elimination (red line, RE), Ni−Et homolytic bond cleavage (blue line, HBC), and nucleophilic attack for oTolN$_3$

dx.doi.org/10.1021/ic501766k | Inorg. Chem. 2014, 53, 11633−11639

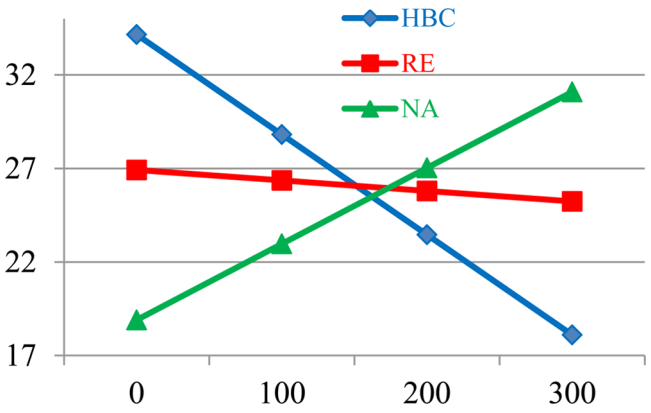

Figure 8. Plot of estimated temperature dependence (*x*-axis, K) of the free energy barriers (*y*-axis, kcal/mol) for butane reductive elimination (red line, RE), Ni−Et homolytic bond cleavage (blue line, HBC), and nucleophilic attack for $oTolN_3$ (green line, NA). HBC = homolytic bond cleavage. RE = reductive elimination.

(green line, NA) indicated that at temperatures up to ∼150 K that NA will dominate, Figure 8. Above ∼200 K, Ni−Et bond scission becomes the dominant pathway. At ∼150 K, all three processes are predicted to compete as each has estimated $\Delta G^{\ddagger}$ ∼ 26 kcal/mol.

Given the Hamiltonian and basis set approximations that were utilized in this research, one expects the slopes and intercepts in Figure 8 to change, but the above graph is thought provoking and yields three predictions. First, the products of the $N_3Ar/bpyNiEt_2$ reaction will be quite sensitive to the temperature used in the synthesis. Second, assuming the "crossing point" of the above lines at ca. 26 kcal/mol as a reasonable estimate, organometallic reactions will dominate over the metal-free processes (see Supporting Information). Third, products derived from radical processes will be more prevalent at higher temperatures, while insertion of "NAr" into the Ni−C bond prefers lower temperatures.

How might radical pathways differentiate the reactivity of mesityl azide with $bpyNiEt_2$ from that of $oTolN_3$, $pTolN_3$, and $mXyN_3$? The calculated BDFEs shed some light on a possible answer to this question, Table 2. Note the similarity in the Ni−N and Ni−Et BDFEs for the unhindered pTol and mXy substitutents, which were of similar magnitude to those of the parent phenyl substituent. There is an obvious reduction in bond strength (∼9 and ∼6 kcal/mol for Ni−N and Ni−Et bonds, respectively) for oTol versus the unhindered substituents, Table 2. *There is a further reduction upon traversing to the bulkiest Mes substituent, and indeed, the favorable entropic contribution for bond scission yields a negative BDFE for the Ni−Et bond of bpyNi(Et)(N(Mes)Et)!* While the degree of uncertainty in these calculations makes quantitative calculation of radical concentrations tenuous, one may reasonably conclude that (a) radicals will be most prevalent in reactions involving the mesityl substituent, and (b) radicals will increase in concentration with increasing temperature. These two factors provide the most plausible explanation for the differing reactivity of MesN3 in that syntheses involving this reagent were pursued at higher temperatures than the other aryl azides. In the larger context of pursuing Earth-abundant 3d metal catalysis, the closeness of odd (radical) and even electron pathways highlights a major challenge for theorists and experimentalists alike.

Table 2. Calculated Bond Dissociation Free Energies (kcal/mol) for bpyNi(Et)(N(Ar)Et) at 298.15 K and 1 atm

Ar	BDFE(Ni−N(Ar)Et)	BDFE(Ni−Et)
Ph	18.5	10.1
pTol	17.8	9.5
oTol	8.6	3.1
mXy	18.0	8.9
Mes	4.0	−2.5

COMPUTATIONAL METHODS

All calculations utilized the Gaussian 09[27] package at the B3LYP/6-31+G(d) level of theory. Unless noted otherwise, all quoted energies are free energies computed at 1 atm and 298.15 K using unscaled vibrational frequencies. Temperature effects in Figure 8 were probed via the estimation of free energies from 0 to 300 K every 100 K All stationary points were characterized as minima or transition states via inspection of the energy Hessian. All optimizations were done without symmetry or internal coordinate restraint. Calculations on closed- and open-shelled species utilized restricted and unrestricted, respectively, Kohn−Sham methods. Where deemed necessary, calculation of the minimum energy crossing points (MECPs) was performed utilizing the code described by Harvey and co-workers.[6] Computed MECPs with the current level of theory (B3LYP/6-31+G(d)) were compared to the much higher level of theory utilized by Besora and Harvey[6] (i.e., MR_AQCC/cc-pVTZ) for the reaction $MeN_3 \rightarrow N_2 + {}^3MeN$; the calculations revealed a negligible difference, <1.0 kcal/mol. Throughout the Article, nonsinglet stationary points are indicated by a superscript prefix numeral.

ASSOCIATED CONTENT

Supporting Information

Free energies of all calculated species along with a full citation for ref 27. Results and discussion for the modeled metal-free reactions of aryl azides. This material is available free of charge via the Internet at http://pubs.acs.org.

AUTHOR INFORMATION

Corresponding Author

*E-mail: tomc@unt.edu.

Notes

The authors declare no competing financial interest.

ACKNOWLEDGMENTS

This article is dedicated to the memory of Professor Gregory L. Hillhouse. We thank Greg for his support and encouragement of this research. T.M.F. acknowledges the support of UNT through a Toulouse Graduate School Fellowship as well as Prof. Dan Ess and Dr. Albin Petit (Chemistry, BYU) for guidance in MECP calculations. T.R.C. thanks the U.S. Department of Energy (Basic Energy Sciences) for support of this research through Grant DE-FG02-03ER15387.

REFERENCES

(1) Matsunaga, P. T.; Hillhouse, G. L.; Rheingold, A. L. *J. Am. Chem. Soc.* **1993**, *115*, 2075−2077.
(2) Matsunaga, P. T.; Hess, C. R.; Hillhouse, G. L. *J. Am. Chem. Soc.* **1994**, *116*, 3665−3666.
(3) Lin, B. L. Ph.D. Dissertation. University of Chicago, 2000.
(4) Yamamoto, T.; Abla, M. *J. Organomet. Chem.* **1997**, *535*, 209−211.
(5) Allen, F. H. *Acta Crystallogr.* **2002**, *B58*, 380−388.
(6) Besora, M.; Harvey, J. N. *J. Chem. Phys.* **2008**, *129*, 044303/1−10.
(7) Kogut, E.; Zeller, A.; Warren, T. H.; Strassner, T. *J. Am. Chem. Soc.* **2004**, *126*, 11984−11994.

(8) Zhao, Y.; Truhlar, D. J. *Acc. Chem. Res.* **2008**, *41*, 157−167.
(9) Mindiola, D. J.; Hillhouse, G. L. *J. Am. Chem. Soc.* **2001**, *123*, 4623−4624.
(10) Waterman, R.; Hillhouse, G. L. *J. Am. Chem. Soc.* **2008**, *130*, 12628−12629.
(11) Kogut, E.; Wiencko, H. L.; Zhang, L.; Cordeau, D. E.; Warren, T. H. *J. Am. Chem. Soc.* **2005**, *127*, 11248−11249.
(12) Wiese, S.; McAfee, J. L.; Pahls, D. R.; McMullin, C. L.; Cundari, T. R.; Warren, T. H. *J. Am. Chem. Soc.* **2012**, *134*, 10114−10121.
(13) Harrold, N. D.; Waterman, R.; Hillhouse, G. L.; Cundari, T. R. *J. Am. Chem. Soc.* **2009**, *131*, 12872−12873.
(14) Lee, S. W.; Trogler, W. C. *Acta Crystallogr.* **1990**, *C46*, 900−901.
(15) Lee, S. W.; Miller, G. A.; Campana, C. F.; Trogler, W. C. *Inorg. Chem.* **1988**, *27*, 1215−1219.
(16) Overbosch, P.; van Koten, G.; Overbeek, O. *Inorg. Chem.* **1982**, *21*, 2373−2378.
(17) Overbosch, P.; van Koten, G.; Spek, A. L.; Roelofsen, G.; Duisenberg, A. J. M. *Inorg. Chem.* **1982**, *21*, 3908−3913.
(18) Figg, T. M.; Cundari, T. R. *Organometallics* **2012**, *31*, 4998−5004.
(19) Hartwig, J. F.; Cook, K. S.; Hapke, M.; Incarvito, C. D.; Fan, Y.; Webster, C. E.; Hall, M. B. *J. Am. Chem. Soc.* **2005**, *127*, 2538−2552.
(20) Tekarli, S. M.; Drummond, M. L.; Williams, T. G.; Cundari, T. R.; Wilson, A. K. *J. Phys. Chem. A* **2009**, *113*, 8607−8614.
(21) Cundari, T. R.; Ruiz-Leza, H. A.; Grimes, T. V.; Steyl, G.; Waters, A.; Wilson, A. K. *Chem. Phys. Lett.* **2005**, *401*, 58−61.
(22) DeYonker, N. J.; Peterson, K. A.; Steyl, G.; Wilson, A. K.; Cundari, T. R. *J. Phys. Chem. A* **2007**, *111*, 11269−11277.
(23) DeYonker, N. J.; Williams, T. G.; Imel, A. E.; Cundari, T. R.; Wilson, A. K. *J. Chem. Phys.* **2009**, *131*, 024106/1−9.
(24) Laskowski, C. A.; Morello, G. R.; Saouma, C. T.; Cundari, T. R.; Hillhouse, G. L. *Chem. Sci.* **2013**, *4*, 170−174.
(25) Brown, S. N.; Mayer, J. M. *J. Am. Chem. Soc.* **1996**, *118*, 12119−12133.
(26) Wolczanski, P. T. *Chem. Commun.* **2009**, *7*, 740−757.
(27) Frisch, M. J.; et al. *Gaussian 09, Revision A.1*; Gaussian, Inc.: Wallingford, CT, 2009.